DESIGNING THE CITY ACCORDING TO THE WIND: USING A CFD TO MINIMIZE THE IMPACTS OF CITY GROWTH ON NATURAL VENTILATION

Renan Cid Varela Leite[1], Anésia Barros Frota[1]
[1]Faculty of Architecture and Urbanism of the University of São Paulo
Laboratory of Environmental Comfort and Energy Efficiency (LABAUT)
Rua do Lago, 876 São Paulo 05508-080, Brazil

ABSTRACT

This research studies the influence of changing patterns of land use on natural ventilation using a cfd tool, with a case study in Fortaleza, Ceará, Brazil. This urban area is intensifying its occupation through tall buildings and constructive densification. Virtual three-dimensional models were reproduced. The first model represents the present situation of this part of the city, the second one expresses the maximum occupancy permitted by urban legislation and a third scenario indicates an intermediate proposal as a criticism of law permissiveness. These models were submitted to the ANSYS CFX 5.6 fluid dynamics software to simulate the airflow. 39 comparison points were used to evaluate the wind field. Results indicated that natural ventilation was prejudiced in the posterior region of the second scenario. However, at local level most of the points of comparison within the maximum occupancy model indicated better ventilation conditions comparing to the intermediate model.

INTRODUCTION

Natural ventilation, where is possible its application, improves indoor air quality by removing pollutants and promotes thermal comfort by accelerating the heat exchange between the body and the surrounding environment.

Mainly in regions of hot and humid climate, where there is a little variation in temperature throughout the day and high levels of humidity, becomes crucial to control the solar radiation and increasing natural ventilation in urban areas and inside the buildings.

Urbanization process structurally modifies natural ventilation as attested by several scientific researches that indicate that disorderly urban growth is responsible for changing local climatic parameters, compromising thermal comfort conditions. These issues are linked to urban planning (Chandler, 1976; Oke, 1987).

Urban form is the result of interactions between building's height, distance between buildings and occupancy rate, changing the permeability of the wind within the urban fabric and influencing its use for passive cooling of buildings.

However, to use the wind for passive cooling of buildings it is necessary to understand the physical phenomenon and the factors that influence natural ventilation process. Currently, the compatibility between verticalization, high-density occupation and maintenance of ventilation in the urban environment is investigated in order to create urban microclimates that never existed in natural conditions. However, the main target is to convert this data into criteria of occupation in urban rates, using such variables to the urban planning process, as Duarte & Serra (2003) attest.

Verifying natural ventilation conditions through models assists the architectural design and urban planning process. Wind tunnel tests, softwares or mathematical models are important tools in the analysis of urban transformations, allowing greater precision in the airflow assessment in internal and external environments, as Prata-Shimomura el al (2009) attest.

Considering natural ventilation as the main passive strategy for thermal comfort in Fortaleza (latitude 3°43' S), it is essential to incorporate it in the densification process of the urban fabric.
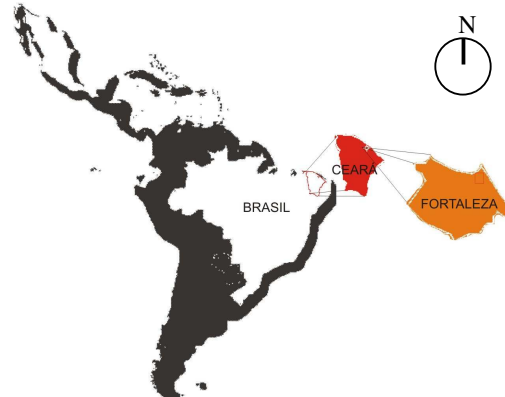

Figure 1 Localization of Fortaleza, Ceará, Brazil

Specifically, the objective of this work is to identify the impacts of tall buildings and constructive densification on natural ventilation over the southeast part of Fortaleza, Ceará, in Brazil, once this sector of the city is experiencing an urban expansion process closely linked to the housing market. Comparing a maximum occupancy scenario with taller buildings and lower occupancy rate allowed by local legislation to the present situation and an intermediate proposal with medium height buildings and higher occupancy

rate, this research verifies the airflow conditions in several points of the study-area.

SIMULATION AND EXPERIMENT

Wind data analysis

Initially, available local wind data collected by the city airport was organized to identify the frequency of occurrence of wind speeds and directions. The data set analyzed is the period between February 12, 2002 and January 30, 2009, a total of 61,032 hours. Within this range, 47,114 of valid records (77% of total hours) were analyzed using the program WRPLOT View 6.5.1. The wind rose plotted determined two predominant wind directions: east and southeast directions with 40% and 37% of total hours. The average speed of the wind blowing from the east is about 3,85 m/s and the southeast wind has 4,51 m/s of average velocity during this period.

Figure 2 Wind rose plotted for 2002-2009 period
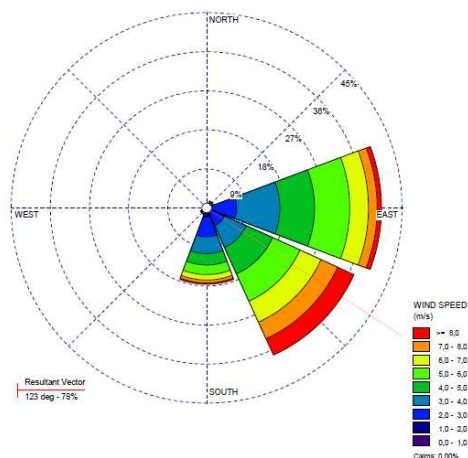
Computational simulation

Computational fluid dynamics softwares, known as CFD tools, are progressively being applied to simulations involving fluids in motion. Currently a wide range of cfd tools is available.

Computational fluid dynamics models are based on Navier-Stokes equations that are solved at all points of a two or three dimensional mesh. The mesh represents the buildings and surrounding areas. In these models, the pressure and velocity are given for determining the initial and boundary conditions (Kolokotronis; Santamouris, 2007).

CFX 5.6 is an example of cfd produced by the ANSYS company that allows the simulation of any situation involving fluid mechanics in any scale and boundary conditions, as long as the computational capacity is provided. The ANSYS CFX 5.6 license availability at the Laboratory of Environmental Comfort and Energy Efficiency (LABAUT) in the Faculty of Architecture and Urbanism of the University of São Paulo and the accumulated experience using this application in other researches also contributed to the choice of this software.

The software consists of 4 modules. In the pre-processing level the geometry is prepared in CAD ambient by determining the model to be adapted in ANSYS ICEM CFD for the development and parameterization of the mesh, defining the points where the equations should be calculated. For the model construction, the buildings are simplified, which reduces considerably the processing time and computational capacity for calculating the simulation.

Then, the definition of the system simulation, equations to be calculated, the initial and boundary conditions and the turbulence model are adopted in CFX-Pre.

The simulation is then calculated in the CFX-Solver and the results are viewed through three-dimensional images and graphics in CFX-Post, inserting points, lines and planes in various locations, allowing the visualization of the airflow in different parts of the model through velocity contours, vectors or streamlines.

Computational geometry

The study reproduced three virtual three-dimensional models. The first model represents the present situation of this part of the city, the second one expresses the maximum occupancy permitted by the current urban legislation in terms of buildings height (72 m) and a lower occupancy rate and a third one indicates an intermediate proposal designed as a criticism of the permissiveness of the law, with building's height about 48 m but with a higher occupancy rate. These three scenarios were submitted to the CFX 5.6 software to simulate the airflow around buildings, allowing the physical phenomena to be captured more accurately and comparing the airflow within the present situation model to the scenarios of maximum and intermediate occupation.

Once only two major wind directions were determined by the wind data analysis, two domains were created to settle each of the three models: an east orientated model and a southeast orientated model. This domain shape allows modelling perpendicular wind directions (90°).

Both computational domains have L X B X H = 2681 X 2104 X 432 m.

Boundary conditions

The definition of boundary conditions is performed by determining characteristics to the domain faces (parts) that will influence the flow.

At the inlet (E and SE wind orientations) of both domains the measured mean wind speed is imposed: 3,85 m/s for the East orientation and 4,51 m/s for the southeast orientation.

Zero static pressure is imposed at the outlet of the domains (W and NW wind orientations).

The top and sidewalls of both domains are modelled as free slip walls (zero normal velocity and zero normal gradients of all variables).

At the ground and building surfaces the standard wall functions used are smooth wall, no slip. This condition (smooth wall) is applied to the sides of buildings and the model floor to represent the typical surfaces of urban environment materials.

The RNG k-ε turbulence model was chosen for this study because of its good performance in predicting the surface pressures on the windward building facades. The flow regime is subsonic and the domain motion option is stationary and non buoyant.
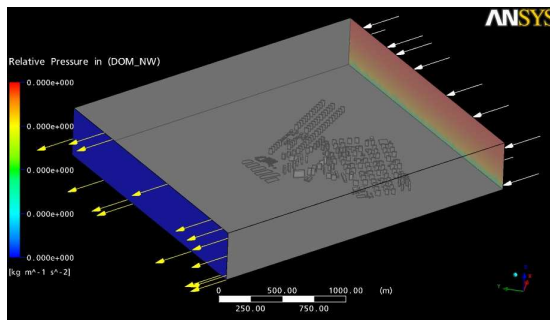

Figure 3 General aspect of the boundary conditions defined for a simulation of the maximum occupancy model with east wind direction.
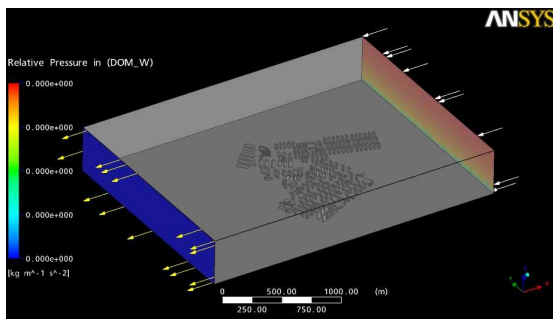

Figure 4 General aspect of the boundary conditions defined for a simulation of the maximum occupancy model with southeast wind direction.

To analyze the airflow within the three models simulated, horizontal planes at different heights were generated. Over these planes velocity vectors and contours were plotted.

The horizontal plane 1 (PH1) is about 1.5 m high, corresponding to the pedestrian level. The second plan (PH2) is at 10 m height, at which the wind data was collected by the weather station located in the city's airport. The third plan (PH3) is located 36 m above the ground, half the maximum height of buildings permitted by law in the study area.

The simulation also used points of comparison distributed along the models for testing and validating the results and velocity vectors in different plans to evaluate the wind field around buildings.

The six simulations reached reliable results according to the convergence criteria recommended by CFX (2003). Their results may be evaluated through the Residual Mean Square (RMS) graphs generated during the simulation calculation. They indicated a RMS about 1×10^{-4}, which is considered regular and enforceable.

DISCUSSION AND RESULT ANALYSIS

East wind analysis

Plotting velocity contours for the east wind simulation over the plans PH1, PH2 and PH3 is possible to analyze specific areas of characteristic stagnant airflow, which are those parts within the models with air speed around 0 and 0.2 m/s. These areas are highlighted in blue colour.

Visualizing the airflow at pedestrian level (1.5 m height) in the maximum occupancy model it is evident that these stagnant areas are located further away from the buildings in the model. The size of the biggest stagnant airflow area is about 4 blocks (400 m), as shown by figure 5.
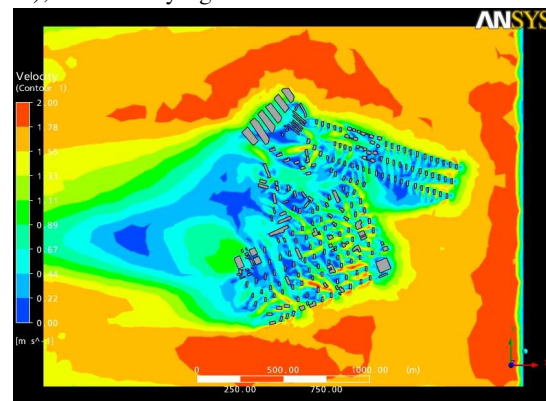

Figure 5 Velocity contours over PH1 (1.5 m height) in maximum occupancy model (E-wind)

On the contrary, in the intermediate model of occupation these areas are located closer to the buildings and appear to be smaller, as shown by figure 6. In addition, there are more areas of stagnant airflow between buildings. This probably occurs because of increase in the land occupancy rate due to the reduction in the height of the buildings.
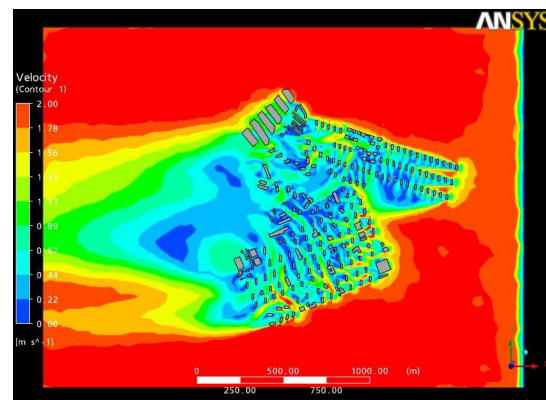

Figure 6 Velocity contours over PH1 (1.5 m height) in intermediate occupancy model (E-wind)

Analyzing the air flow in the maximum occupancy model about 10 m above the ground (PH2) it is

visible the establishment of two major stagnant areas after the buildings in the model, as seen on figure 7.
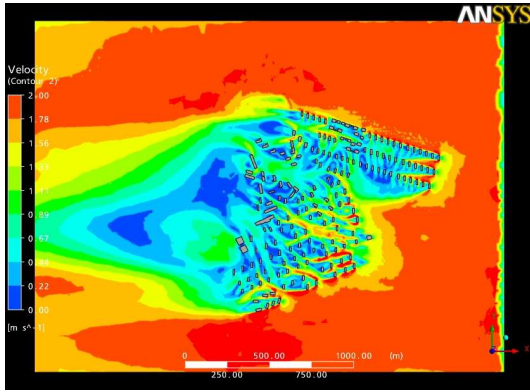

Figure 7 Velocity contours over PH2 (10 m height) in maximum occupancy model (E-wind)

In the intermediate model the decrease in the vortices after the buildings is perceived. More specifically, at the area close to the buildings located in the centre of the model a dilution of the flow is observed. Within this area air velocities are about 0-0.2 m/s (figure 8).

Figure 8 Velocity contours over PH2 (10 m height) in
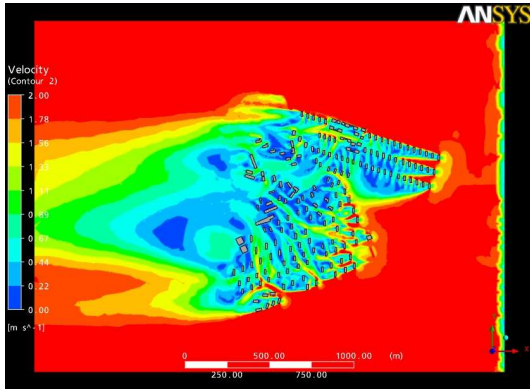
intermediate occupancy model (E-wind)

Comparing the maximum occupancy model to the intermediate model at a horizontal plane 36 m above the ground (PH3), the effects of the buildings over natural ventilation are the same. However, it is quite evident the size reduction of the vortex created after the buildings in the intermediate model.
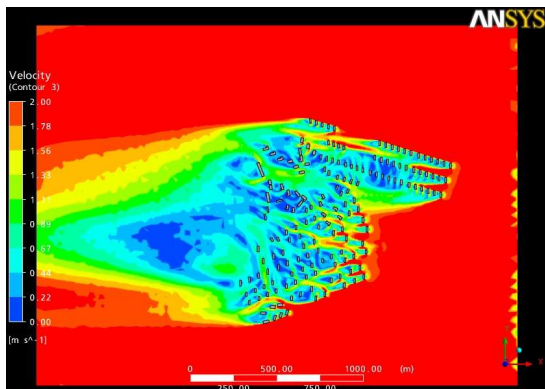

Figure 9 Velocity contours over PH3 (36 m height) in maximum occupancy model (E-wind)

As shown by figure 10, the biggest vortex created by buildings in the intermediate occupancy model is diluted in three smaller areas of slower airflow.
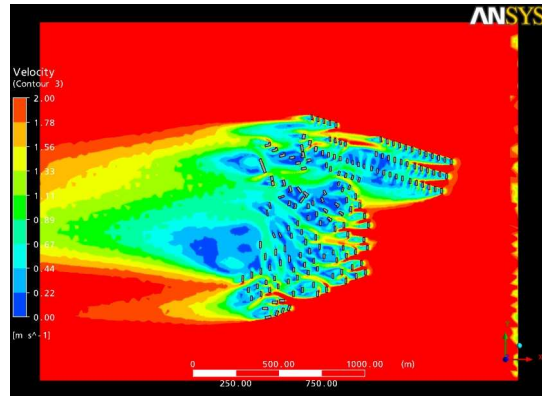

Figure 10 Velocity contours over PH3 (36 m height) in intermediate occupancy model (E-wind)

The streamlines also indicated the change in the flow caused by the tallest buildings in the centre of both models. The buildings act as a barrier to the wind, creating a vortex zone and a turbulence flow after those buildings.

Yet, the increase in the flow velocity at higher levels of the maximum occupancy model has structural impacts on air circulation at the windward facade of the buildings due to the elevation of the wind gradient over this part of the city.
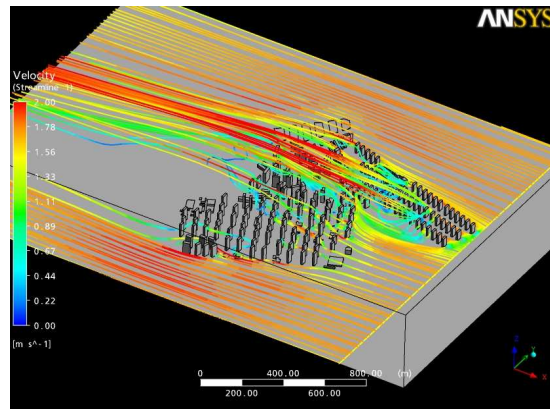

Figure 11 Using streamlines to visualize the airflow over the maximum occupancy model (E-wind)

In the intermediate scenario is interesting to notice that the streamlines do not rise as much as in the maximum occupancy model. This aspect shows that the presence of buildings of 48 m height has less impact on the vortex creation than the arrangement of buildings of 72 m height.
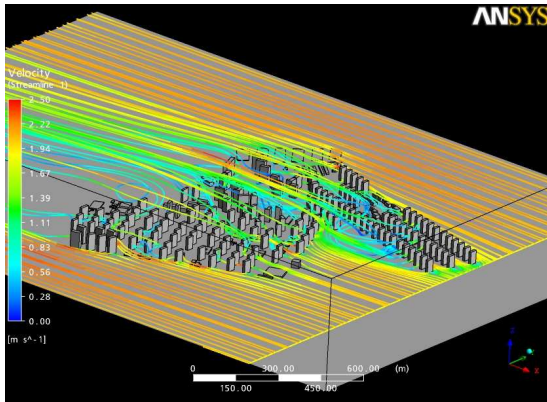
Figure 12 Using streamlines to visualize the airflow over the intermediate occupancy model (E-wind)

Southeast wind analysis

In the simulations of the southeast wind direction the most significant effect of the buildings over the air circulation is the canalization effect of the airflow between buildings and over the streets. This spatial configuration reduces the creation of low air velocities areas within the model's first buildings.

However, despite the canalization effect, a vortex of larger proportions in both models of maximum and intermediate occupation is created. Comparing to the simulations with east wind, the effect over the windward facade is quite evident as shown by the area highlighted in blue (air velocities between 0 – 0,2 m/s) in figures 13 and 14.
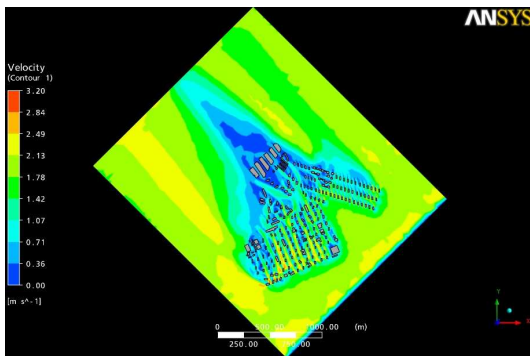

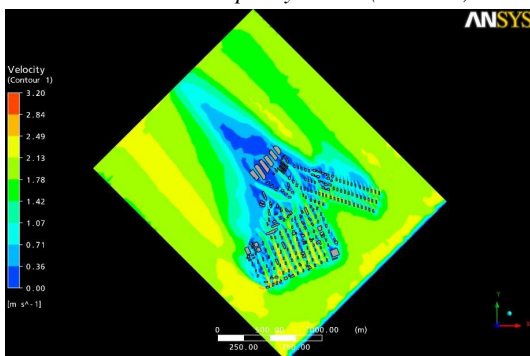*Figure 13 Velocity contours over PH1 (1,5m height) in maximum occupancy model (SE-wind)*

Figure 14 Velocity contours over P1 (1,5m height) in intermediate occupancy model (SE-wind)

With a more spaced occupation adopted by the maximum occupancy model once the higher buildings induce the narrowing of its forms, a division of the main vortex is verified at 10 m above the ground (PH 2). This land occupation seems to minimize the negative effect over the wind at the windward facade when the wind is coming from the southeast, as shown by figure 15.
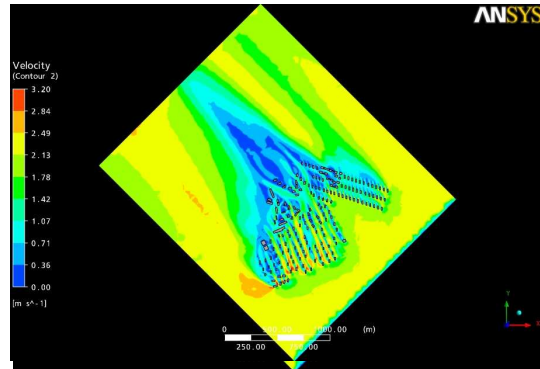

Figure 15 Velocity contours over PH2 (10 m height) in maximum occupancy model (SE-wind)

On the contrary, in the intermediate stage of occupation, despite the presence of lower buildings, the area of stagnant air at 10 m height (PH 2) is markedly larger and concentrated comparing to the maximum occupancy scenario, which represents a significant decrease in air speeds at the windward facades.
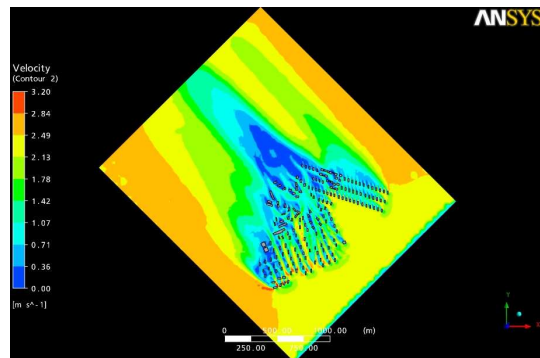

Figure 16 Velocity contours over PH2 (10 m height) in intermediate occupancy model (SE-wind)

Finally, analyzing the airflow at 36 m height (PH3) the stagnant flow area appears to be stretched, narrower in the case of the maximum occupancy model, while in the intermediate scenario that area seems to be a more concentrated form.

At the centre of the intermediate scenario a few stretches with speeds below 1.0 m/s are checked. The generation of small vortices within this model is due to the increased rate of land use.

In the model of maximum occupancy, the area with air velocities below 0,6 m/s is located far from the buildings, being mostly located in the downwind devoid of obstacles. In the intermediate model of occupation, in turn, the vectors in this range are

located right next to buildings. However its aspect seems to be diluted, generating smaller areas of stagnant airflow.
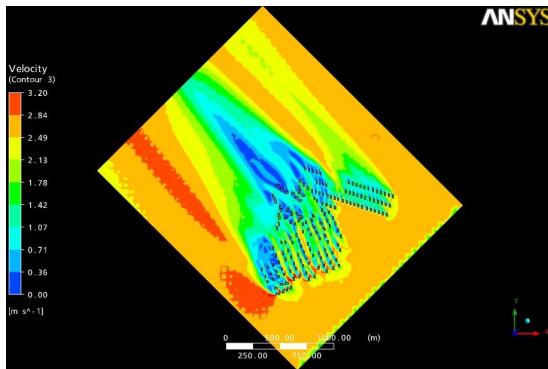

Figure 17 Velocity contours over PH (36 m height) in maximum occupancy model (SE-wind)
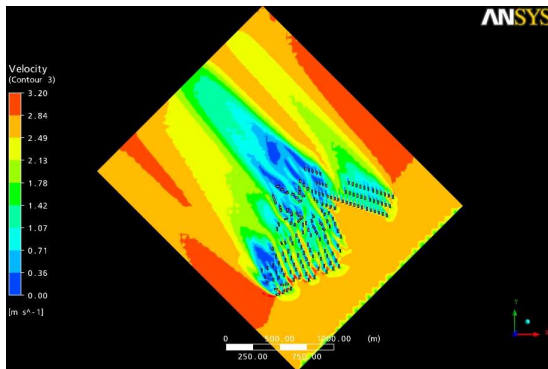

Figure 18 Velocity contours over PH3 (36 m height) in intermediate occupancy model (SE-wind)

As occurred in the simulation with the east wind orientated models, the streamlines identified the increase of the flow velocity at higher levels of the maximum occupancy model due to the height of buildings in this scenario. Once the wind passes through buildings of 16 floors before deviate the 24 buildings within this model the result is the elevation of the wind gradient as shown in figure 19.
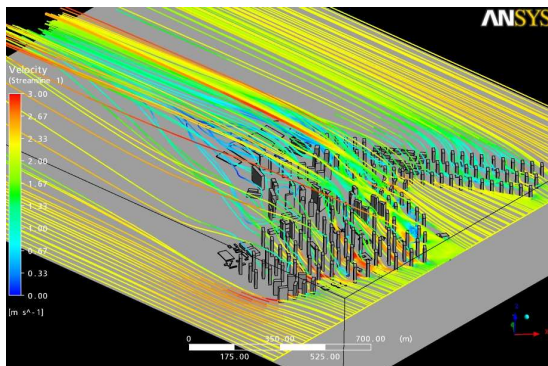

Figure 19 Using streamlines to visualize the airflow over the maximum occupancy model (SE-wind)

In the intermediate model of occupation the higher velocity streamlines occur when entering the area between the buildings. Analogously to the scenario of maximum occupancy, the vortices are characterized as areas in which the turbulent streamlines undergo major deviations and revolutions.

Unlike the maximum occupancy model, in this intermediate occupancy scenario an elevation in the airflows is not that evident. The general airflow remains, in general, slightly above the top of the buildings, as shown in figure 20.
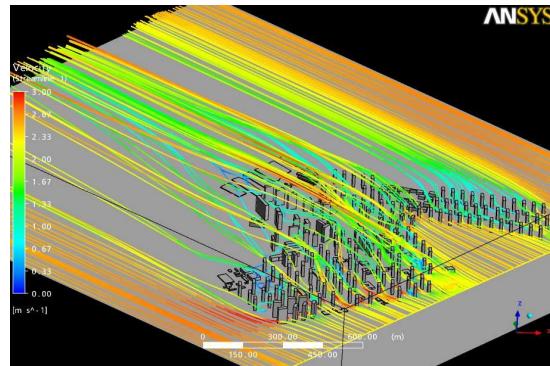
Figure 20 Using streamlines to visualize the airflow over the intermediate occupancy model (SE-wind)

Using comparison points to evaluate the airflow

The velocity profiles according to the height were measured at points of comparison located on the streets and at the centre of blocks as a way to compare the different roughness imposed to the airflow in both scenarios of maximum and intermediate occupancy and present situation.

Figure 21 Localization of comparison points 1, 2, 3, 4 and 5 in the maximum occupancy model (E-wind)

In points 1 and 2 of both maximum and intermediate occupancy models, the wind flow has the same characteristics at the peak up to 10 m, corresponding to a reduction around 30% in P1 and P2 in 70%, compared with the situation current.

Table 1
Air velocities registered in the points of comparison
1, 2, 3, 4 and 5 at different heights

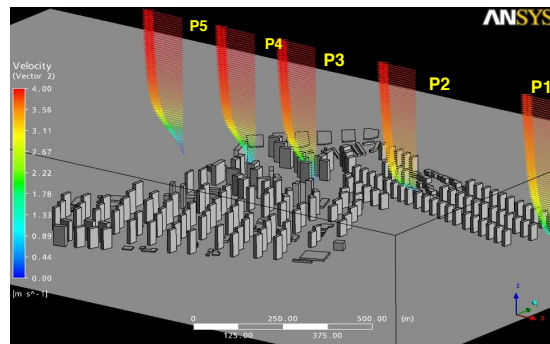| POINT OF COMPARISON 1			
MODEL	PH 1	PH 2	PH 3
Present situation	1,81 m/s	2,02 m/s	2,33 m/s
Maximum occupation	1,09 m/s	1,34 m/s	1,90 m/s
Intermediate occupation	1,32m/s	1,58 m/s	1,92 m/s
POINT OF COMPARISON 2			
MODEL	PH 1	PH 2	PH 3
Present situation	1,67 m/s	1,86 m/s	2,27 m/s
Maximum occupation	0,47 m/s	0,44 m/s	0,33 m/s
Intermediate occupation	0,56 m/s	0,62 m/s	0,44 m/s
POINT OF COMPARISON 3			
MODEL	PH 1	PH 2	PH 3
Present situation	1,37 m/s	1,50 m/s	1,89 m/s
Maximum occupation	0,45 m/s	0,50 m/s	0,85 m/s
Intermediate occupation	0,20 m/s	0,31 m/s	0,70 m/s
POINT OF COMPARISON 4			
MODEL	PH 1	PH 2	PH 3
Present situation	0,62 m/s	0,85 m/s	0,56m/s
Maximum occupation	0,61 m/s	0,71 m/s	0,69 m/s
Intermediate occupation	1,31 m/s	0,98 m/s	0,87 m/s
POINT OF COMPARISON 5			
MODEL	PH 1	PH 2	PH 3
Present situation	0,69 m/s	0,62 m/s	0,40 m/s
Maximum occupation	0,30 m/s	0,19 m/s	0,44 m/s
Intermediate occupation	0,18 m/s	0,12 m/s	0,46 m/s

The velocity profile generated for point 7 already indicates the influence of the change in roughness observed in the stretch. Points 8 and 9 are now placed in a high constructive density area. Point 10 is used to assess the impacts on air movement in the downwind area.
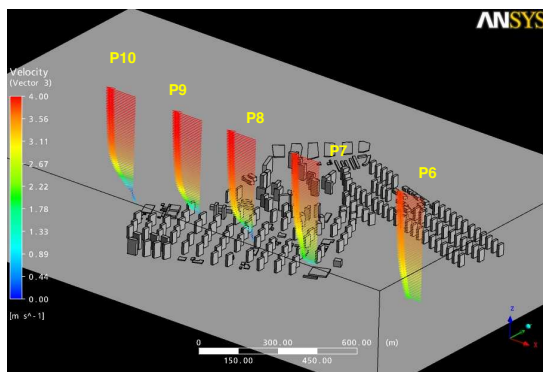

Figure 22 Localization of comparison points 6, 7, 8, 9 and 10 in the intermediate occupancy model (E-wind)

The decreases of air velocities at these points indicate the greatest reduction in that stretch when compared to the present situation model, with airflows about 65% to 95% slower in the lower layers.
From the point 7 and beyond the reduction in the wind intensity in both models of denser land occupation are quite evident comparing to the present situation. More specifically, the significant decrease

of air velocities at lower levels of maximum occupancy scenario shows that the increase in buildings dimensions to 72 m has a major impact on the local wind patterns.

Table 2
Air velocities registered in the points of comparison
6, 7, 8, 9 and 10 at different heights

POINT OF COMPARISON 6			
MODEL	PH 1	PH 2	PH 3
Present situation	2,01 m/s	2,16 m/s	2,37 m/s
Maximum occupation	1,55 m/s	1,86 m/s	2,23 m/s
Intermediate occupation	1,91m/s	2,23 m/s	2,30 m/s
POINT OF COMPARISON 7			
MODEL	PH 1	PH 2	PH 3
Present situation	1,75 m/s	2,05 m/s	2,42 m/s
Maximum occupation	0,48 m/s	0,79 m/s	1,82 m/s
Intermediate occupation	0,92 m/s	1,35 m/s	2,09 m/s
POINT OF COMPARISON 8			
MODEL	PH 1	PH 2	PH 3
Present situation	1,00 m/s	1,67 m/s	2,39 m/s
Maximum occupation	0,15 m/s	0,20 m/s	0,14 m/s
Intermediate occupation	0,74 m/s	0,58 m/s	0,16 m/s
POINT OF COMPARISON 9			
MODEL	PH 1	PH 2	PH 3
Present situation	1,25 m/s	1,51 m/s	2,30m/s
Maximum occupation	0,40 m/s	0,42 m/s	0,33 m/s
Intermediate occupation	0,81 m/s	0,91m/s	0,72 m/s
POINT OF COMPARISON 10			
MODEL	PH 1	PH 2	PH 3
Present situation	1,50 m/s	1,71 m/s	2,17 m/s
Maximum occupation	0,92 m/s	0,92 m/s	0,69 m/s
Intermediate occupation	0,71 m/s	0,63 m/s	0,30 m/s

Similarly to the measurement of velocity profiles in the present situation model, at points P11 and P12 the air velocity seems to remain close to the values recorded in present scenario. Reductions in these locations are situated around 10% slower in the maximum occupancy model.
However, in other points the flow begins to suffer the interference of a higher roughness. At points 3 and 4 the reduction reaches higher values.
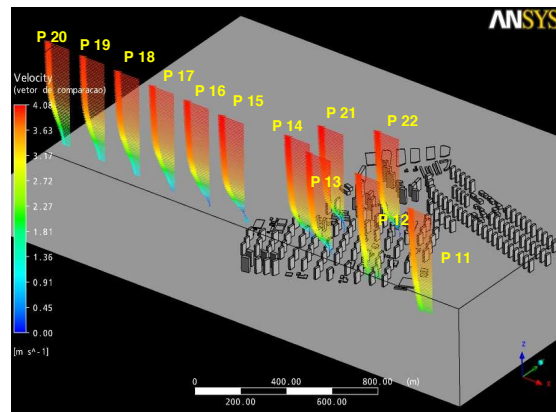

Figure 23 Localization of comparison points 1, 2, 3, 4 and 5 in the maximum occupancy model (E-wind)

POINT OF COMPARISON 11			
MODEL	**PH 1**	**PH 2**	**PH 3**
Present situation	2,12 m/s	2,16 m/s	2,37 m/s
Maximum occupation	1,60 m/s	1,85 m/s	2,18 m/s
Intermediate occupation	1,85m/s	2,12 m/s	2,31 m/s
POINT OF COMPARISON 12			
MODEL	**PH 1**	**PH 2**	**PH 3**
Present situation	1,73 m/s	2,14 m/s	2,40 m/s
Maximum occupation	1,80 m/s	2,10 m/s	1,72 m/s
Intermediate occupation	1,40 m/s	1,72 m/s	2,17 m/s
POINT OF COMPARISON 13			
MODEL	**PH 1**	**PH 2**	**PH 3**
Present situation	1,12 m/s	1,88m/s	2,47 m/s
Maximum occupation	0,56 m/s	0,60 m/s	0,45 m/s
Intermediate occupation	0,86 m/s	0,89 m/s	0,51 m/s
POINT OF COMPARISON 14			
MODEL	**PH 1**	**PH 2**	**PH 3**
Present situation	0,83 m/s	1,31 m/s	2,31 m/s
Maximum occupation	0,04 m/s	0,03 m/s	0,16 m/s
Intermediate occupation	0,44 m/s	0,52 m/s	0,55 m/s
POINT OF COMPARISON 15			
MODEL	**PH 1**	**PH 2**	**PH 3**
Present situation	0,89 m/s	1,32 m/s	2,30 m/s
Maximum occupation	0,98 m/s	0,99 m/s	0,94 m/s
Intermediate occupation	0,78 m/s	0,79 m/s	0,50 m/s
POINT OF COMPARISON 16			
MODEL	**PH 1**	**PH 2**	**PH 3**
Present situation	2,00 m/s	2,05 m/s	2,27 m/s
Maximum occupation	0,65 m/s	0,61 m/s	0,25 m/s
Intermediate occupation	0,23 m/s	0,25 m/s	0,44 m/s
POINT OF COMPARISON 17			
MODEL	**PH 1**	**PH 2**	**PH 3**
Present situation	2,01 m/s	2,06 m/s	2,29 m/s
Maximum occupation	0,25 m/s	0,23 m/s	0,35 m/s
Intermediate occupation	0,66 m/s	0,72 m/s	0,96 m/s
POINT OF COMPARISON 18			
MODEL	**PH 1**	**PH 2**	**PH 3**
Present situation	2,02 m/s	2,07 m/s	2,31 m/s
Maximum occupation	0,45 m/s	0,50 m/s	0,68 m/s
Intermediate occupation	0,92 m/s	1,00 m/s	1,19 m/s
POINT OF COMPARISON 19			
MODEL	**PH 1**	**PH 2**	**PH 3**
Present situation	1,91 m/s	2,07 m/s	2,30m/s
Maximum occupation	0,73 m/s	0,78 m/s	0,91 m/s
Intermediate occupation	2,30 m/s	0,91m/s	1,30 m/s

The points of comparison 32, 33 and 34 in the models of maximum and intermediate occupancy are set in high built density ares into the southeast wind direction simulations. The consequence of such conditions is the reduction of 50% to 70% in air velocities below 50 m height when compared to the present situation.

In the intermediate model, over the entire downwind area (points 35 to 39) the intensity of the airflow suffers little reductions comparing to the present situation. The disruption of the wind speed reaches values of 5% to 15% lower than those registered in the present situation. On the contrary, in the maximum occupancy scenario reductions of 18% to 35% are registered.
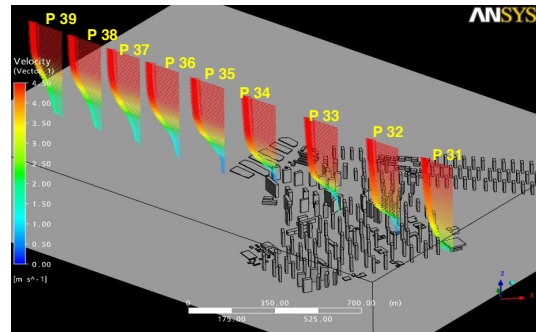

Figure 24 Localization of comparison points 31 to 39 in the maximum occupancy model (SE-wind)

CONCLUSION

The largest reductions of air velocity were verified in the maximum occupancy model. Comparing to the intermediate occupation model results, all the points of comparison in the downwind area of the buildings registered lower speeds, with air velocity values from 30% to 90% slower than the present situation model.

The simulation results corroborate with the assumption that the verticalization of the city and a lower occupancy rate allow better air circulation within the city fabric since this urban form is more permeable to the wind. On the other hand, the elevation of the urban canopy layer and the reduction of the air velocity at the immediately posterior regions are the main effects of this urban form.

Although the study of natural ventilation conditions should be considered at specific conditions of each locality, since the conditions of air circulation are easily changed by the construction parameters, this research might help urban design process specifically in parts of the city in constructive densification process, indicating that, despite the increase in height, the higher land use rates may cause the stagnation of the airflow even if it is associated with lower building's height.

ACKNOWLEDGEMENT

REFERENCES

CFX, 2003. CFX 5 Solver Models. Diddcot Oxfordshire.

CHANDLER, T. J. 1976. Urban Climatology and its Relevance to Urban Design. Geneva, WMO. Technical Note 149.

DUARTE, D. H. S., SERRA, G. G. 2003. Padrões de ocupação do solo e microclimas urbanos na região de clima tropical continental brasileira: correlações e proposta de um indicador. ANTAC Magazine. Porto Alegre, v. 3, n. 2, p. 7-20, abr./jun.

KOLOKOTRONI, M; SANTAMOURIS, M. 2007. Ventilation for cooling. In: Advances in passive cooling. SANTAMOURIS, M. (org.) Buildings, Energy, Solar Techonolgy, London UK.

OKE, T. R. 1987. Boundary Layer Climates. 2 ed. London: Methuen.

PRATA-SHIMOMURA, A.; FROTA, A. B.; CELANI, G. 2009. Modelos físicos na análise de ventilação urbana: o uso do túnel de vento. FÓRUM vol. 3, no. 2. Belo Horizonte, Brazil.